Interaction of Calcineurin and Type-A GABA Receptor γ_2 Subunits Produces Long-Term Depression at CA1 Inhibitory Synapses

Jian Wang,[1]* ShuHong Liu,[1]* Ursula Haditsch,[2] WeiHong Tu,[1] Kimberley Cochrane,[1] Gholamreza Ahmadian,[3] Linda Tran,[1] Jadine Paw,[1] YuTian Wang,[3] Isabelle Mansuy,[2] Michael M. Salter,[4] and YouMing Lu[1]

[1]Neuroscience Research Group, Department of Physiology and Biophysics, Faculty of Medicine, University of Calgary, Calgary, Canada, T2N 4N1, [2]Institute of Cell Biology, Swiss Federal Institute of Technology, CH-8093 Zürich, Switzerland, and Departments of [3]Pathology and [4]Physiology, Programme in Brain and Behaviour, Hospital for Sick Children, University of Toronto, Toronto, Canada, M5G 1X8

Long-term depression (LTD) is an activity-dependent weakening of synaptic efficacy at individual inhibitory synapses, a possible cellular model of learning and memory. Here, we show that the induction of LTD of inhibitory transmission recruits activated calcineurin (CaN) to dephosphorylate type-A GABA receptor ($GABA_A$Rs) via the direct binding of CaN catalytic domain to the second intracellular domain of the $GABA_A$R-γ_2 subunits. Prevention of the CaN–$GABA_A$ receptor complex formation by expression of an autoinhibitory domain of CaN in the hippocampus of transgenic mice blocks the induction of LTD. Conversely, genetic expression of the CaN catalytic domain in the hippocampus depresses inhibitory synaptic responses, occluding LTD. Thus, an activity-dependent physical and functional interaction between CaN and $GABA_A$ receptors is both necessary and sufficient for inducing LTD at CA1 individual inhibitory synapses.

Key words: **$GABA_A$ receptors; inhibitory synapses; plasticity; dephosphorylation; calcineurin; hippocampus**

Introduction

In CA1 neurons of the hippocampus, field stimulation of Schaffer-collateral fibers evokes diphasic excitatory–inhibitory synaptic currents: a fast EPSC mediated by AMPA receptors followed by a fast IPSC (Lu et al., 2000). A brief high-frequency stimulation (tetanus) of the Schaffer-collateral fibers produces long-term potentiation (LTP) of EPSCs and concomitantly long-term depression (LTD) of IPSCs (Andersen and Lømo, 1968; Stelzer et al., 1987; Lu et al., 2000). These coordinately regulated bidirectional changes of the excitatory and inhibitory synaptic strength are considered to be a cellular model of learning and memory (Bliss and Collingridge, 1993; Paulsen and Moser, 1998). Although we now know a great deal about the molecular steps contributing to the induction of LTP at excitatory synapses (Malenka and Nicoll, 1999; Malinow et al., 2000; Ali and Salter, 2001; Lisman and Zhabotinsky, 2001), the molecular mechanisms underlying the induction of LTD at CA1 individual inhibitory synapses have not been identified (Abraham et al., 1987; Thompson and Gahwiler, 1989; Thompson, 1994; Aizenman et al., 1998).

Fast IPSCs in CA1 neurons are mediated predominantly by type-A GABA receptors ($GABA_A$Rs) (MacDonald and Olsen, 1994). The induction of LTD of $GABA_A$ receptor-mediated IPSCs ($GABA_A$R-IPSCs) requires activation of excitatory NMDA receptors (Stelzer et al., 1987). The biochemical links between the NMDA receptors and the pathway for inducing LTD of $GABA_A$R–IPSCs involve calcineurin (CaN) (Lu et al., 2000). CaN, or Ca^{2+}/calmodulin-dependent phosphatase 2B, consists of a 61 kDa catalytic domain (CaN-A) and a 19 kDa regulatory subunit (CaN-B) (Cohen, 1989). The enzymatic activity of CaN in CA1 neurons of the hippocampus is increased by activation of NMDA receptors (Lu et al., 2000). Also, there is extensive evidence showing that CaN plays a critical role in the activity-dependent changes of excitatory synaptic transmission in the hippocampus (Winder and Sweatt, 2001). Genetic inhibition of endogenous CaN in the forebrain (CaN transgenic mice), by expressing the auto-inhibitory domain of CaN, showed that LTP at CA1 excitatory synapses induced by subsaturating but not saturating tetanic stimulation was enhanced both *in vitro* and *in vivo* (Malleret et al., 2001). In another line of experiments, transgenic mice (CN98 transgenic mice) were generated in which a catalytic domain of CaN (CaN-Aα) was expressed in the forebrain (Winder et al., 1998). In these animals, NMDA receptor-dependent LTP induced by weak tetanus in the CN98 mutant mice was no different from that seen in control mice, but LTP elicited by stronger tetanus was reduced in CN98 mutant mice. These data suggest that manipulations of CaN activity alter the ability of CA1 excitatory synapses to induce LTP.

Because CaN downregulates $GABA_A$ receptor function (Chen and Wong, 1995), activated CaN may interact with the synaptic $GABA_A$ receptors for NMDA receptor-dependent LTD at CA1 inhibitory synapses. A direct test of this hypothesis has not yet been undertaken. Thus, we used double whole-cell patch-clamp recordings to induce LTD at CA1 individual

Received Aug. 16, 2002; revised Nov. 14, 2002; accepted Nov. 15, 2002.

This work was supported by the Canadian Institute for Health Research (Y.M.L), Heart and Stroke Foundation, Canada (Y.M.L), Alberta Heritage Foundation for Medical Research (Y.M.L), Canada Foundation for Innovation (Y.M.L), and Alberta Foundation for Innovation and Science (Y.M.L). We thank Dr. Brian Perrino for the construct of CaN420. We thank Drs. John F. MacDonald, Wayne Giles, Keith Sharkey, and Brian MacVicar, for critical comments on this manuscript.

*J.W. and S.L. contributed equally to this work.

Correspondence should be addressed to Dr. YouMing Lu, Department of Physiology and Biophysics, Faculty of Medicine, University of Calgary, Calgary, Canada, T2N 4N1. E-mail: luy@ucalgary.ca.

 0270-6474/03/230826-11$15.00/0

inhibitory synapses. By taking advantage of a combined molecular genetic and biochemical approach, we demonstrate that NMDA receptor-dependent physical and functional interaction between CaN-A and $GABA_AR$-γ_2 subunit ($GABA_AR\gamma_{2S}$) fulfills necessary and sufficient conditions for inducing LTD of inhibitory transmission.

Materials and Methods

Double whole-cell patch-clamp recordings and LTD induction. Hippocampal slices (300 μm) were prepared from 30 ±2-d-old CaN transgenic control or mutant mice for Figures 1–4 and from 34 ±3-d-old CN98 transgenic mice for Figures 6 and 7. CaN mutant mice were generated by expressing the autoinhibitory domain in the C terminus of CaNα in the forebrain with the doxycycline-dependent reverse tetracycline-controlled transactivator system, resulting in a 35–45% decrease in CaN activity. For all experiments, doxycycline (Mutual Pharmaceutical, Philadelphia, PA) was administered at 6 mg/g food at least 1 week before experimentation. Control mice were treated with dox only, as described in detail previously (Malleret et al., 2001). The slices were prepared as described previously (Lu et al., 1998, 2000). All procedures were in compliance with and approved by the University Animal Care and Use Committee, University of Calgary. For double whole-cell patch-clamp recordings from CA1 interneuron and pyramidal cell pairs, hippocampal slices were visualized with infrared (IR) illumination and a differential interference contrast (DIC) Axioskop 2FS plus equipped with Hamamatsu C2400–07E optics (see Fig. 1*A*). A whole-cell recording (tight-seal >1 GΩ) with patch electrode (3–5 MΩ) was initially obtained from a CA1 interneuron at the border of stratum radiatum and lacunosum-moleculare (LM). Subsequently, the second whole-cell recordings (tight-seal >10 GΩ) were established from a CA1 pyramidal cell. The synaptic connections between CA1 interneurons and pyramidal cells were also identified by *post hoc* morphological analysis (see Fig. 1*A*). Single spikes in interneurons triggered unitary IPSCs in pyramidal cells that were blocked by the $GABA_A$ receptor antagonist bicuculline (10 μM). An extracellular stimulating electrode was placed at the CA1 Schaffer-collateral fibers. LTD was induced by tetanus (two 100 Hz stimuli lasting 1 sec at an intertrain interval of 10 sec) of the Schaffer-collateral fibers. The unitary $GABA_AR$–IPSCs were filtered at 5 kHz with a low-pass filter. Data were digitized at a frequency of 10 kHz and stored on-line using the pclamp8 system. The input resistance and series resistance in postsynaptic pyramidal cells were monitored using prevoltage steps (−2 mV, 100 msec) at 5 min intervals throughout the period of the experiment. Series resistance ranged from 9 to 12 MΩ. Input resistance was 328 ± 29 MΩ. For current-clamp mode, the intracellular solution contained (in mM): 115 K^+-gluconate, 7.5 K^+Cl, 27.5 K^+-methylsulfate, 10 HEPES, 0.2 EGTA, 2 Mg-ATP, 0.3 guanosine triphosphate, and 0.1% biocytin, pH 7.4, 296 mOsm. For voltage-clamp recordings, the low Cl^- solution contained (in mM): 142.5 Cs-gluconate, 7.5 CsCl, 10 HEPES, 0.2 EGTA, 2 Mg-ATP, and 0.3 guanosine triphosphate, pH 7.4, 296 mOsm, and the high Cl^- solution contained (in mM): 150 CsCl, 10 HEPES, 0.2 EGTA, 2 Mg-ATP, 0.3 guanosine triphosphate, and 0.1% biocytin, pH 7.4, 296 mOsm.

Coimmunoprecipitation, affinity purification ("pull-down"), and Western blotting. The CA1 region was microdissected as described previously (Lu et al., 1998). Four CA1 regions from control or LTD (5 or 30 min after induction of LTD) were pooled and homogenized in ice-cold lysis buffer containing 50 mM Tris-HCl, pH 7.6, 150 mM NaCl, 1% NP-40, 2 mM EDTA, 1 mM sodium orthovanadate, and proteinase inhibitor mixture (Sigma, St. Louis, MO) (5 μl/100 mg tissue). After clearing debris by centrifuging at 14,000 × *g* at 4°C, protein concentration in the extracts was determined by Bradford assay (Bio-Rad, Hercules, CA). The extracts (~500 μg protein) were incubated with nonspecific IgG (2 μg) or polyclonal mouse anti-CaN-A (2 μg; PharMingen, San Diego, CA) with or without 10 μg anti-CaN-A immunizing antigen (peptide I^{457}-P^{482}; PharMingen) overnight at 4°C, followed by the addition of 40 μl of Protein G-Sepharose (Sigma) for 3 hr at 4°C. In the immunoprecipitations with polyclonal rabbit antibody against $GABA_AR$-α_1 subunit (anti-α_1, 2 μg; Upstate BioTechnology, Lake Placid, NY), the anti-α_1 was cross-linked to the protein G-Sepharose. This previous cross-linking of the anti-α_1 permits the elution of antigen only to prevent interference of the IgG subunits in blotting (He et al., 1995). Cross-linking was performed with 0.5% glutaraldehyde (30 min, 25°C). The reaction was then terminated and washed four times with lysis buffer. The extracts (~500 μg protein) were then incubated with the cross-linked anti-α_1 with or without 10 μg immunizing antigen (a peptide corresponding to residues 1–15 of the α_1 subunit) (Upstate Biotechnology). Immunoprecipitates were washed four times with lysis buffer and denatured with SDS sample buffer and separated by 12% SDS-PAGE. Proteins were transferred onto nitrocellulose membranes using a Bio-Rad mini-protein-III wet transfer unit overnight at 4°C. Transfer membranes were then incubated with blocking solution [5% nonfat dried milk dissolved in TBST buffer (pH 7.5, 10 mM Tris-HCl, 150 mM NaCl, and 0.1% Tween 20)] for 1 hr at room temperature, washed three times, and incubated with monoclonal rabbit primary antibody against CaN-A (1:1000), polyclonal rabbit antibodies against $GABA_AR$-α_1 subunit (anti-α_1, 1:1000; Alpha Diagnostic), $GABA_AR$-β_2 subunit (anti-β_2, 1:1000; Alpha Diagnostic), or $GABA_AR$-γ_2 subunit (anti-γ_2, 1:2000; Alpha Diagnostic) for 1 hr at room temperature. Membranes were washed three times with TBST buffer and incubated with the appropriate secondary antibodies (1:1000 dilution) for 1 hr followed by washing four times. Signal detection was performed with an enhanced chemiluminescence kit (Amersham Biosciences, Arlington, IL). The lanes marked "input" were loaded with 10% of the starting material used for immunoprecipitation. The precipitated bands were semiquantified using "the normalizing method" of the Densitometer Quantity One (see Quantity One User Guide, Bio-Rad). The intensities of the lanes marked input in each gel were normalized as 100%. Each of the other bands in the same gel was then expressed as the percentage of the respective input.

Glutathione *S*-transferase (GST) fusion proteins of $GABA_AR$-$\alpha_1^{334-420}$ (GST-α_1), -$\beta_2^{327-451}$ (GST-β_2), -$\gamma_{2S}^{317-442}$ (GST-γ_{2S}), -$\gamma_{2S}^{332-442}$ (*GST-γ_{2S}), and -$\gamma_{2S}^{317-332}$ (short form) were prepared from bacterial lysates as described in detail previously (Liu et al., 2000). The extracts (~200 μg of proteins) were incubated with the indicated GST fusion proteins (~100 μg of protein), with or without 200 μg of γ_2 peptide, overnight at 4°C, and then for another 3 hr at 4°C after 20 μl of Protein G-Sepharose (Sigma) was added. Beads were washed five times with lysis buffer. Eluted proteins were incubated in sample buffer (final concentration 5% SDS) and subjected to SDS-PAGE (12% gel). Transferred proteins were revealed by Western blot. In the experiments of Figure 3, *E* and *F*, the transferred membranes were incubated with monoclonal mouse primary antibody against α-adaptin (1:1000; CN Biosciences) and monoclonal mouse antibodies against Src (1:1000; Upstate Biotechnology) for 1 hr at room temperature. Signal detection was performed with an enhanced chemiluminescence kit (Amersham Biosciences).

In vitro *binding assays*.CaN420 (10 μg/ml) or CaN-B subunit (10 μg/ml) was incubated overnight at 4°C in 0.5 ml containing 40 mM Tris-HCl, pH 7.5, 0.5 mM $CaCl_2$, 150 mM 2-mercaptoethanol, 0.2 mg/ml BSA, 40 μl glutathione-Sepharose beads (Pharmacia), and 10 μg GST-α_1, GST-β_2, GST-γ_{2S}, or *GST-γ_{2S}. In some assays, as indicated in Figure 3, 10 μg/ml γ_2-peptide or scrambled γ_2-peptide (Biosynthesis Inc.) was included. The amino acid sequence of scrambled γ_2-peptide was LDHSYFKVNDRDKPKK; it was created by random ordering of the sequence of γ_2-peptide, LHYFVSNRKPSKDKDK, corresponding to the 317–332 residues of the $GABA_A$ receptor γ_2 subunit. The beads were washed five times with 200 μl PBS containing 0.1% Triton X-100 and eluted twice with 20 μl glutathione elution buffer. Eluted proteins were incubated in sample buffer (final concentration 5% SDS) and subjected to SDS-PAGE (12% gel). Transferred proteins were revealed by Western blot. Expression and purification of CaN420 and CaN-B were described in detail previously (Perrino et al., 1995).

The γ_2 subunit phosphorylation assay. Rabbit polyclonal anti-γ_2pSer^{327} antibodies were raised against phospho-γ_2 peptide (^{317}LHYFVSNRKP(p)SKDKDK^{332}). The resulting antisera were then affinity purified with phospho-γ_2 peptide immobilized on Affigel 10 (Bio-Rad). This antibody is competitively blocked with antigen peptide (see Fig. 5*B*). The $GABA_A$ receptors were immunoprecipitated by previous cross-linked polyclonal rabbit anti-γ_2 from CA1 hippocampal extracts, as described above. Precipitated $GABA_A$ receptors and the *in vitro* phosphorylated GST-γ_{2S} and

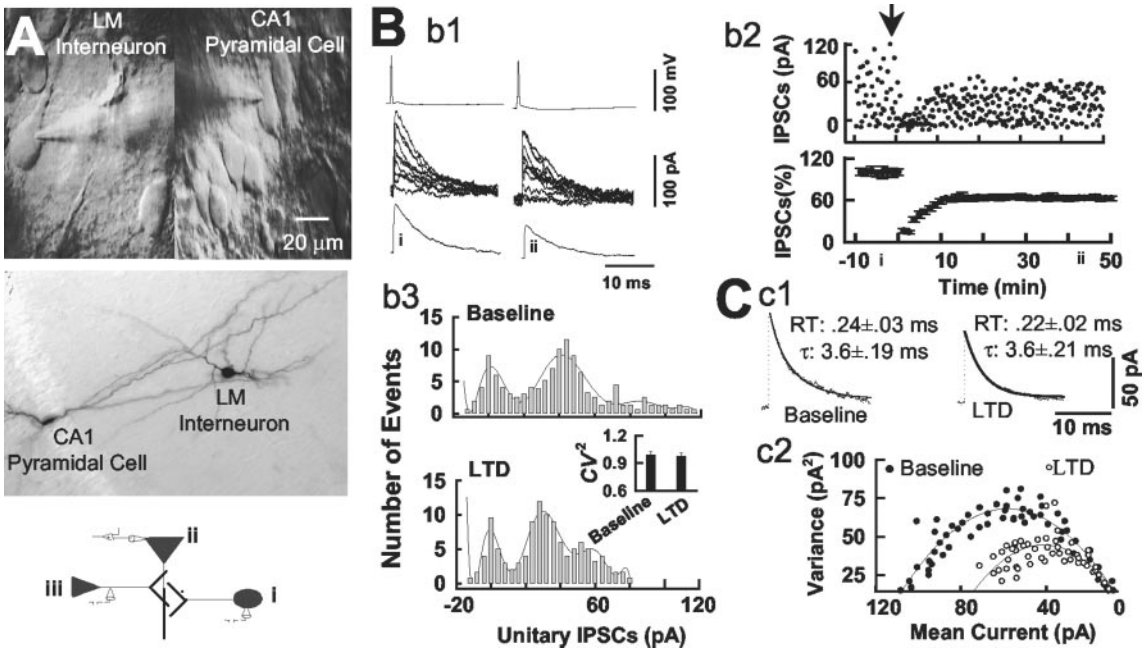

Figure 1. Induction of LTD at CA1 individual inhibitory synapses. *A*, IR-DIC images of double patch pipette tips on a lacunosum-moleculare (*LM*) interneuron and a pyramidal cell in a hippocampal slice (*left*). Shown are the morphology (*middle*) of a synaptically connected LM interneuron and a pyramidal cell pair labeled with biocytin and the arrangement (*bottom*) of the electrodes at a LM interneuron (*i*) paired with a pyramidal cell (*ii*) and an extracellular stimulating electrode at the Schaffer-collateral fibers (*iii*). *B*, Induction of LTD of the unitary $GABA_A$R–IPSCs. *b1*, Single action potentials (*top*) and 10 consecutive single (*center*) and averaged $GABA_A$R–IPSCs (*bottom*) at −60 mV are taken before (*i*) and after (*ii*) tetanus. *b2*, A representative recording (*top*) and the averaged amplitudes (*bottom*) of the unitary $GABA_A$R–IPSCs are plotted. *b3*, Amplitude distribution histograms for the unitary $GABA_A$R–IPSCs before (*Baseline*) and 20 min after tetanus (*LTD*) are plotted with bin sizes of 4 pA. *Inset*, Summarized coefficient variance ($CV^{-2} = M^2/\sigma^2$; $n = 10$ cells/5 control mice). *C*, The number of open channels of the synaptic $GABA_A$ receptors was reduced during LTD. *c1*, Ten to 90% rise time (*RT*) and time constants (τ) of decay before and after the induction of LTD were unchanged. *c2*, Current–variance relationships for the unitary $GABA_A$R–IPSCs are plotted before (*Baseline*) and during LTD. The data points are fitted by a parabolic function ($\sigma^2 = iI_m - I_m^2/N_o$), where σ^2 is the variance, I_m is the mean current, i is the single channel current, and N_o is the number of synaptically activated channels.

the GST-γ_{2S} mutant (Ser^{327}-Ala) (see below) were subjected to SDS-PAGE (12% gel). Transferred proteins were incubated with rabbit polyclonal anti-$\gamma_2 pSer^{327}$ (1:500) for 1 hr at room temperature. Signal detection was performed with an enhanced chemiluminescence kit (Amersham Biosciences).

The GST-α_1, GST-β_2, GST-γ_{2S}, or GST-γ_{2S} mutant (Ser^{327}-Ala) or GST alone (200 μg/each), was incubated with 1 μg/ml protein kinase C (PKC), catalytic fragment (BioMol Research Laboratories), protein kinase Aα catalytic subunit (BioMol Research Laboratories), and 0.4 mM [γ^{32}P]-ATP (1000 cmp/pmol), or the same concentration of ATP (see Fig. 5*A*), in 20 mM HEPES, pH 7.5, 10 mM $MgCl_2$, 0.5 mM $CaCl_2$, 10% glycerol, 5 μg/ml diolein, for 5 min at 30°C. The products were incubated with 10 μg of beads for 1 hr at room temperature and washed five times with 200 μl of PBS. The ^{32}P-labeled GST-α_1, GST-β_2, GST-γ_{2S} beads were then resuspended in phosphatase assay buffer, which contained 40 mM Tris-HCl, pH 8.0, 0.1 M NaCl, 0.4 mg/ml bovine serum albumin, 1 mM dithiothreitol, and 0.45 μM okadaic acid and incubated at 30°C for 1 min in buffer. In Figure 5*A*, the phosphorylated GST-γ_{2S} and the GST-γ_{2S} mutant (Ser^{327}-Ala) were subjected to SDS-PAGE (12% gel).

Results

Induction of LTD of the unitary $GABA_A$R–IPSCs at CA1 inhibitory synapses

LTD of the unitary $GABA_A$R–IPSCs was recorded at CA1 interneuron–pyramidal cell synapses, using double whole-cell patch-clamp recordings with an IR-DIC optic system (Fig. 1*A*). As shown in Figure 1*B*, 30 min after tetanus, the amplitude of the unitary $GABA_A$R–IPSCs decreased to 68.2 ± 7.4% (mean ± SEM) of baseline ($n = 10$ cells/5 control mice). This decrease was maintained over the course of 1 hr recordings.

To determine whether LTD was presynaptic or postsynaptic in origin, we estimated the unitary $GABA_A$R–IPSC variability by computing the inverse of the square of the coefficient variance ($CV^{-2} = M^2/\sigma^2$) (Edwards et al., 1990; Silver et al., 1998), where M is the mean unitary $GABA_A$R–IPSCs, and σ is the variance about M. In accordance with previous observations (Nusser et al., 1998), the distribution of the unitary $GABA_A$R–IPSCs at the baseline (baseline noise: −3 ± 4.1 pA; $n = 10$ cells/5 control mice) has several clearly distinguishable peaks. The distribution was fitted by the sum of multiple Gaussian functions with one peak centered at 0 mV (failures) and other skewed peaks. The induction of LTD produced a shift in the distribution of the unitary $GABA_A$R–IPSCs toward smaller amplitude values, with no change in the number of the failures (Fig. 1*B*). The mean unitary $GABA_A$R–IPSC amplitude (M) is reduced after the induction of LTD, whereas the CV obtained by the method of M^2/σ^2 is unchanged (Fig. 1*B*). The data indicate that a decrease in the postsynaptic $GABA_A$ receptor function may underlie LTD at CA1 inhibitory synapses.

To determine whether a decrease in the channel conductance (γ) of the synaptic $GABA_A$ receptors or a decrease in the number (N_o) of synaptically activated channels contributes to LTD, we performed nonstationary fluctuation analysis (non-SFA) (Traynelis et al., 1993; De Koninck and Mody, 1994; Otis et al., 1994; Auger and Marty, 1997) for the experiments in Figure 1*B* ($n = 10$ cells/5 animals). We first analyzed the kinetic properties of the averaged unitary $GABA_A$R–IPSCs. As can be seen in Figure 1*C*, no changes of the unitary $GABA_A$R–IPSCs rise times or their decay time constants (τ) were observed after the induction of LTD. The average responses were then scaled to the peak and subtracted from individual unitary $GABA_A$R–IPSCs. The variance of the fluctuation around mean was calculated and plotted

against mean currents (Fig. 1*C*). The data points were fit by a parabolic function ($\sigma^2 = iI_m - I_m^2/N_o$), where σ^2 is the variance, I_m is the mean current, i is the single channel current, and N_o is the number of open channels of synaptic $GABA_A$ receptors. At the baseline, estimated γ was 24.2 ± 3.6 pS, which was not significantly different from that (23.6 ± 3.8 pS) during LTD ($p > 0.50$; $n = 10$ cells/5 mice). Estimated γ is close to previously reported values of 20–32 pS for estimates of γ derived from noise analysis in hippocampal granule cells (De Koninck and Mody, 1994; Nusser et al., 1998). In contrast, a significant decrease in N_o during LTD was observed; the synapses have on average 51 ± 7.2 (mean ± SEM; $n = 10$) open channels on the baseline, and this number decreased to 36 ± 4.8 (mean ± SEM; $n = 10$ cells) after the induction of LTD. The data suggest that the average number of open channels of the synaptic $GABA_A$ receptor channels is reduced during LTD.

LTD recruits CaN-A to form a complex with $GABA_A$ receptors

To explore the mechanisms underlying reduction in the number of open $GABA_A$ receptor channels during LTD, we explored the physical interaction of endogenous CaN and $GABA_A$ receptors. We immunoprecipitated extracts of control (Fig. 2*A*) and LTD-CA1 slices using antibodies against either CaN-A (anti-CaN-A) or the $GABA_A$ receptor-α_1 subunit (anti-α_1). We found that 5 and 30 min after the induction of LTD, $GABA_A$ receptor-α_1, -γ_2, and -β_2 subunits, the predominant $GABA_A$ receptor subunits expressed in hippocampus (McKernan and Whiting, 1996), were coimmunoprecipitated with anti-CaN-A. Conversely, CaN-A was immunoprecipitated with anti-α_1 (Fig. 2*B*). A nonspecific IgG did not immunoprecipitate either CaN-A or $GABA_A$ receptors. In control CA1 extracts, however, no coimmunoprecipitation of CaN-A or $GABA_A$ receptors was observed with either antibody (Fig. 2*A*), indicating that the induction of LTD recruits CaN-A into the $GABA_A$ receptor complex.

The major intracellular loops of the $GABA_A$ receptor subunits contain many consensus phosphoserine/threonine residues (Moss et al., 1992; Brandon et al., 1999, 2000), which may be targeted by CaN-A. To investigate this possibility, we constructed GST fusion proteins encoding the second intracellular loops $\alpha_1^{334-420}$, $\beta_2^{327-451}$, and $\gamma_{2S}^{317-442}$ (short form) of the $GABA_A$ receptors. These fusion proteins precipitated CaN-A from the LTD-CA1 extracts but not from controls (Fig. 3*A*). The data suggest that synaptic activity drives activated CaN into the $GABA_A$ receptor complex. The $GABA_A$ receptor fusion proteins may bind indirectly to the activated CaN and directly to their respective subunit to pull down CaN-A from the CaN-A-$GABA_A$ receptor complex in the CA1 extracts.

We then determined whether CaN-A directly binds to $GABA_A$ receptors. We generated a constitutively expressed recombinant CaN catalytic fragment (CaN420) that exhibits stable Ca^{2+}-independent phosphatase activity (Perrino et al., 1995). The GST fusion proteins encoding $\alpha_1^{334-420}$, $\beta_2^{327-451}$, $\gamma_{2S}^{317-442}$, and $\gamma_{2L}^{317-446}$ subunits of the $GABA_A$ receptors were incubated with either CaN420 or CaN-B. As shown in Figure 3*B*, the CaN420, but not CaN-B, bound to GST-$\gamma_{2S}^{317-442}$ and $\gamma_{2L}^{317-446}$, but not to GST alone, or α_1- or β_2-peptide fusion proteins. A GST–$GABA_A$ receptor-γ_{2S} deletion mutant (GST-$\gamma_{2S}^{332-442}$ or *GST-γ_{2S}) failed to bind CaN420, indicating the importance of residues 317–332 within the γ_2 subunit for direct interaction with CaN-A. This was confirmed with a synthesized γ_2-peptide encoding residues 317–332 of the γ_2 subunit, which prevented binding of CaN420 to GST-γ_{2S} (Fig. 3*B*). Consistent with this, we also found

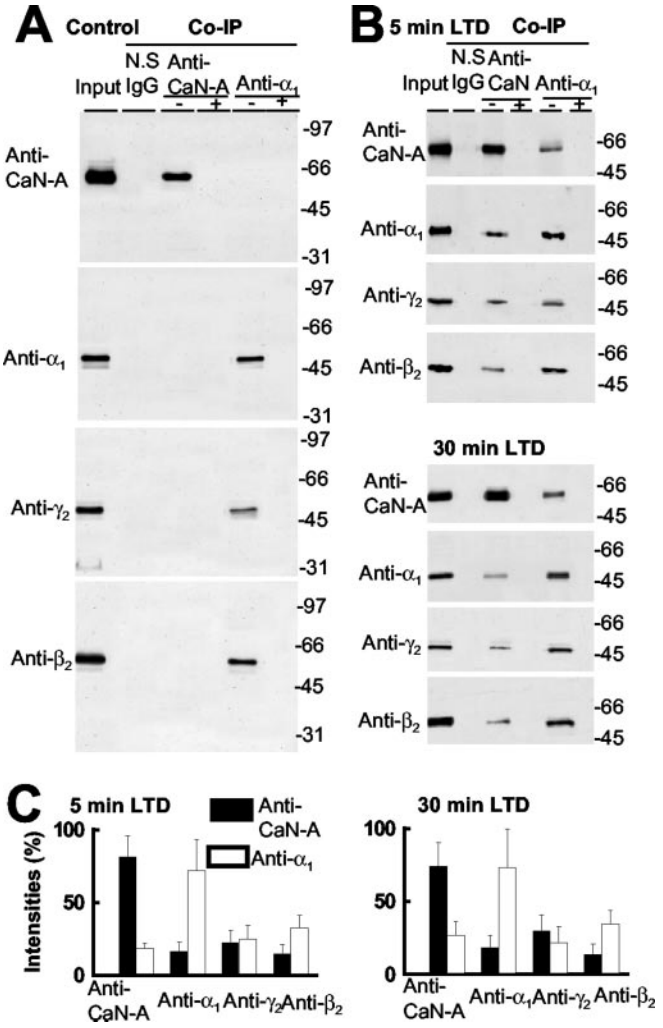

Figure 2. LTD recruits CaN-A to form a complex with $GABA_A$ receptors. *A*, *B*, Immunoprecipitation of the CA1 slices, 30 min after control stimulation (*A*) or 5 and 30 min after the induction of LTD (*B*), with nonspecific (*N.S.*) mouse IgG or a polyclonal mouse anti-CaN-A with (+) or without (−) 10 μg of immunizing antigen (a peptide corresponding to residues 457–482 of CaN), and a previous cross-linked anti-α_1 (see Materials and Methods) with (+) or without (−) 10 μg of immunizing antigen (a peptide corresponding to residues 1–15 of α_1 subunit). Blots were probed with monoclonal rabbit anti-CaN-A or rabbit anti-α_1, anti-γ_2, or anti-β_2, as indicated. In the lane marked *Input*, 50 μg of proteins without immunoprecipitation was loaded. The molecular size is marked at the *right* of the each *panel*. *C*, Immunoprecipitates were quantified for anti-CaN-A (*filled bars*) and anti-α_1 (*open bars*). Each immunoprecipitated band was normalized as a percentage of the respective input. Error bars are ±SEM ($n = 4$).

that CaN-A can bind to GST-$\gamma_2^{317-332}$ (Fig. 3*C*) and that γ_2-peptide interfered with $GABA_A$ receptor-CaN-A association in the LTD CA1 extracts (Fig. 3*D*).

It is known that synaptic $GABA_A$ receptor function is regulated by tyrosine kinase Src and adaptin α and β subunits of AP2 (Kittler et al., 2000; Brandon et al., 2001) and that Src- and adaptin-γ_2 subunit interaction increases the synaptic $GABA_A$ receptor activity. Thus, CaN may have acted as a competitive inhibitor of these molecules to downregulate the $GABA_A$ receptor function. To investigate this, we examined whether γ_2-peptide interferes with Src- and adaptin-$GABA_A$ receptor association. Consistent with previous studies, we found that $GABA_A$ receptor fusion proteins precipitated the endogenous Src (Fig. 3*E*) and α-adaptin (Fig. 3*F*) in the CA1 extracts. In the presence of γ_2 peptide, α-adaptin but not Src can still be precipitated. The data

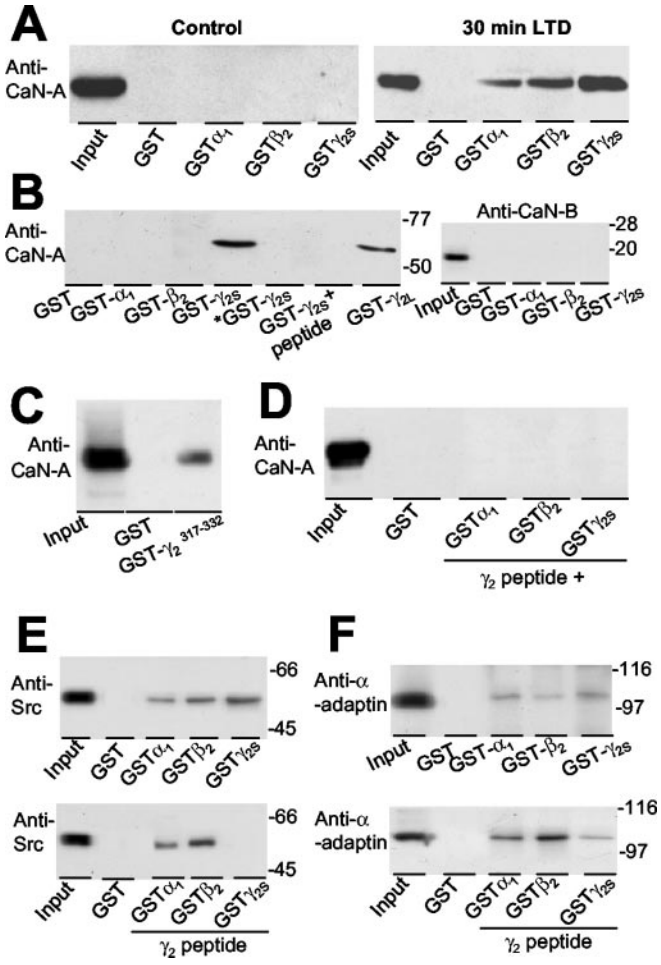

Figure 3. Direct binding of CaN-A to the second intracellular domain of γ_2 subunit. *A*, Affinity precipitation of the CA1 extracts, 30 min after control stimulation, or the induction of LTD, with GST-α_1, GST-β_2, GST-γ_{2S}, or GST alone, and blots were probed with anti-CaN-A. *B*, Direct binding of CaN-A to GST-γ_2. CaN420 (1 μg) or CaN-B (1 μg) was incubated with 10 μg of GST-α_1 or GST-β_2, GST-γ_{2S}, *GST-γ_{2S}, or GST-γ_{2S} + 10 μg γ_2-peptide, or GST-γ_{2L} (long form) or GST alone, and blots were probed with anti-CaN-A or anti-CaN-B, as indicated. *C*, CaN-A binds to GST-$\gamma_2^{317-332}$. *D*, Affinity precipitation of the LTD-CA1 extracts with 10 μg of GST-α_1, GST-β_2, GST-γ_{2S}, or GST alone, in the presence of 10 μg of γ_2-peptide, and blots were probed with anti-CaN-A. *E*, Affinity precipitation of the CA1 extracts with GST-α_1, GST-β_2, GST-γ_{2S}, or GST alone (*top*) or in the presence of γ_2 peptide (*bottom*), and blots were probed with anti-Src, as indicated. *F*, Affinity precipitation of the CA1 extracts with GST-α_1, GST-β_2, GST-γ_{2S}, or GST alone (*top*) or in the presence of γ_2 peptide (*bottom*), and blots were probed with anti-α-adaptin, as indicated. Similar results are observed in each of four experiments ($n = 4$). The molecular size is marked at the *right* of the each *panel*.

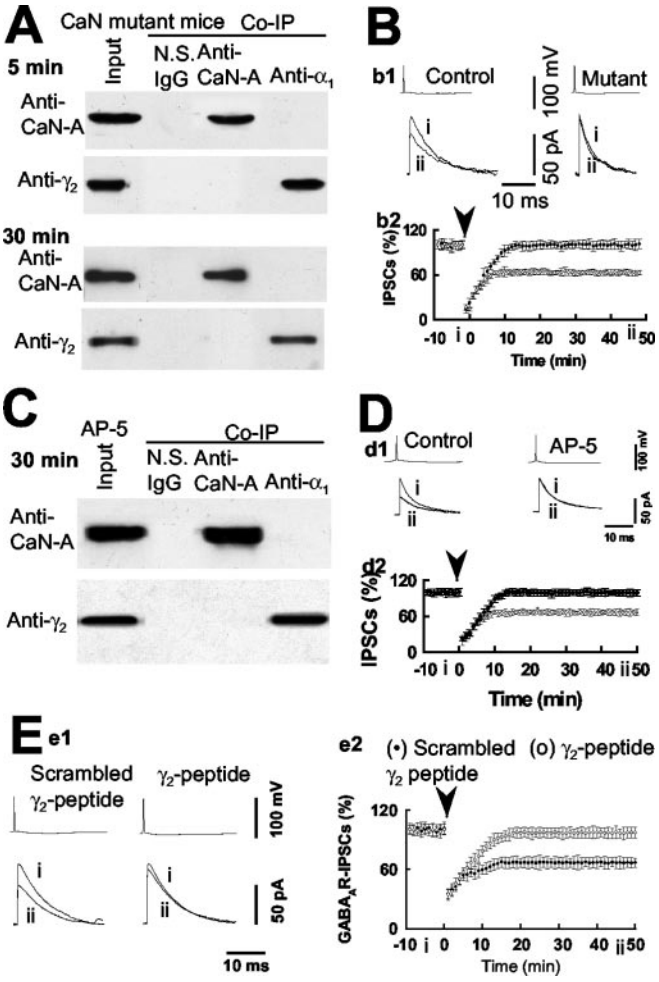

Figure 4. Blockade of CaN-A–$GABA_A$ receptor complex formation prevents the induction of LTD. *A*, Immunoprecipitation of the CaN mutant CA1 slices, 5 and 30 min after tetanus, with an N.S. IgG or anti-CaN-A or anti-α_1. Blots were probed with anti-CaN-A or anti-γ_2. In the lane marked *Input*, 50 μg of proteins without immunoprecipitation was loaded. Similar results are observed in each of the four experiments. *B*, LTD is abolished in the CaN mutant mice. *b1*, Single action potentials (*top*) and averaged unitary $GABA_A$R–IPSCs at −60 mV (*bottom*) are taken before (*i*) and after (*ii*) tetanus (*arrowhead*). *b2*, The averaged amplitudes of the unitary $GABA_A$R–IPSCs are plotted for the experiments with CaN control (*open circles*; the same as in Fig. 1*B*) or CaN mutant mice (*filled circles*). *C*, Immunoprecipitation of the CaN control mice CA1 slices, after tetanus in the presence of 50 μM AP-5, with an N.S. IgG or anti-CaN-A or anti-α_1. Blots were probed with anti-CaN-A or anti-γ_2. *D*, Induction of LTD depends on NMDA receptors. *d1*, Single action potentials (*top*) and averaged unitary $GABA_A$R–IPSCs at −60 mV (*bottom*) are taken before (*i*) and after (*ii*) tetanus (*arrowhead*). *d2*, Normalized unitary $GABA_A$R–IPSCs are plotted for the recordings with the control (*filled circles*; $n = 5$) or AP-5 (*open circles*; $n = 6$). *E*, γ_2-peptide blocks the induction of LTD. *e1*, Single action potentials (*top*) and averaged unitary $GABA_A$R–IPSCs at −60 mV (*bottom*) are taken before (*i*) and after (*ii*) tetanus (*arrowhead*). *e2*, Normalized unitary $GABA_A$R–IPSC amplitudes are plotted for the experiments with γ_2-peptide (*open circles*; $n = 8$) or scrambled γ_2-peptide (*filled circles*; $n = 7$).

suggest that Src may also bind to residues 317–332 of the γ_2 subunit.

CaN-A-$GABA_A$ receptor complex formation is necessary for LTD

To test whether this activity-dependent interaction between CaN-A and $GABA_A$ receptors is essential for the induction of LTD at CA1 individual inhibitory synapses, we examined the consequence of blocking CaN-A-$GABA_A$ receptor complex formation. First, we blocked endogenous CaN by expressing a peptide corresponding to the autoinhibitory domain in the C terminal of CaN-Aα in the hippocampus of transgenic mice (Malleret et al., 2001). No interaction between CaN-A and $GABA_A$ receptors could be observed 5 and 30 min after tetanus in the CaN mutant mice (Fig. 4*A*), and the effect of the tetanus on the unitary $GABA_A$R–IPSCs was completely abolished in mutant mice in that the unitary $GABA_A$R–IPSCs 30 min after tetanus was 93 ± 10.6% of baseline (Fig. 4*B*) ($n = 10$ cells/5 animals). Second, blockade of the CaN-A-$GABA_A$ receptor complex formation by an NMDA receptor antagonist, AP-5 (Fig. 4*C*), prevented the induction of LTD of the unitary $GABA_A$R–IPSCs (Fig. 4*D*). Third, we applied 10 μM γ_2-peptide directly into the CA1 postsynaptic pyramidal cells and found that it abolished LTD of the unitary $GABA_A$R–IPSCs (Fig. 4*E*). A peptide with the same amino acid composition, but in random order, scrambled γ_2-peptide, served as a control, and did not prevent induction of LTD. Thus, NMDA

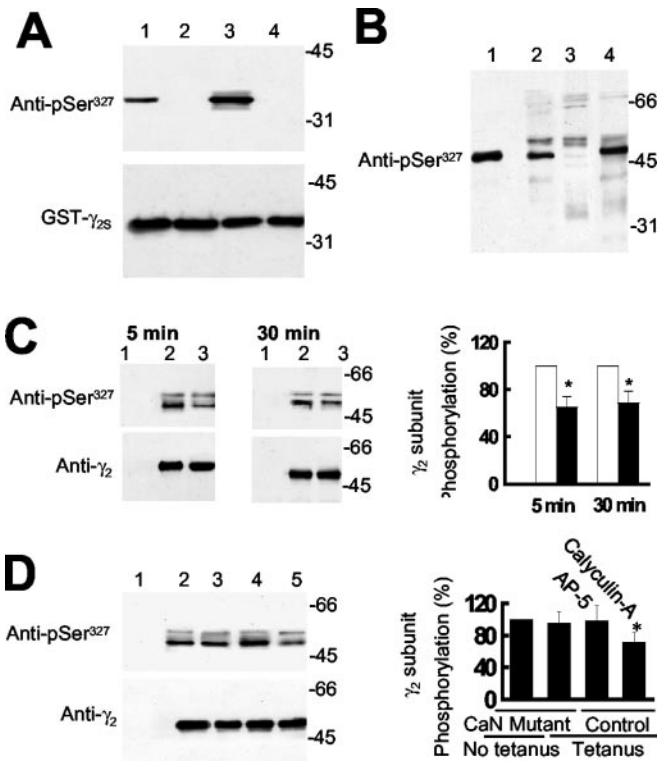

Figure 5. CaN-A and LTD dephosphorylate $GABA_A$ receptors. *A*, Protein immunoblot of phosphorylated $GABA_A$ receptors using anti-γ_2pS^{327}. *Top*, The GST-γ_{2S} (*lanes 1*, *3*) or the mutant GST-γ_{2S} (Ser^{327}-Ala) (*lanes 2*, *4*) were subjected to *in vitro* phosphorylation for 1 min (*lanes 1*, *3*) or 5 min (*lanes 2*, *4*). *Bottom*, Blot of SDS-PAGE by anti-GST antibody. *B*, Immunoblot of SDS-PAGE after precipitation by previous cross-linked polyclonal rabbit anti-γ_2 (see Materials and Methods) from CA1 slices with either a rabbit polyclonal anti-γ_2, as indicated (*lane 1*), or anti-γ_2pS^{327} without (*lane 2*) or with phosphopeptide antigen (*lane 3*) or nonphosphopeptide (*lane 4*). *C*, Anti-γ_2pS^{327} immunoblots of SDS-PAGE after precipitation by N.S. IgG (*lane 1*) or anti-γ_2 from CA1 slices 5 and 30 min after control stimulation (*lane 2*) or the induction of LTD (*lane 3*). The precipitates were quantitated for γ_2 subunit phosphorylation. The levels of γ_2 subunit phosphorylation after induction of LTD (*filled bars*) were normalized to their respective *lane 2* (control stimulation; *open bars*). Error bars are ±SEM ($n = 4$; *$p < 0.01$). *D*, The anti-γ_2pS^{327} (*top*) and anti-γ_2 (*bottom*) immunoblots of SDS-PAGE after precipitation by N.S. IgG (*lane 1*) or anti-γ_2 from the CaN mutant slices without tetanus (*lane 2*) or with tetanus (*lane 3*) or the CaN control mice with tetanus in the presence of AP-5 (*lane 4*) or calyculin-A (*lane 5*). Data were normalized to *lane 2* from the same gel in *bar graph*. *$p < 0.01$ ($n = 5$); paired Student's *t* test.

receptor-dependent interaction of activated CaN and $GABA_A$ receptors was required for induction of LTD at CA1 inhibitory synapses.

CaN-A and LTD dephosphorylates $GABA_A$ receptor γ_2 subunits

The CaN-A–$GABA_A$ receptor complex formation may strategically position the CaN catalytic domain to dephosphorylate synaptic $GABA_A$ receptors. It is now known that CaN-A directly interacts with residues 317–332 within the γ_2 subunit that contains a phosphoserine (pSer^{327}) residue. We therefore developed a phosphospecific antibody to pSer^{327} γ_2 peptide (anti-γ_2pSer^{327}) to analyze LTD-dependent changes in $GABA_A$ receptor γ_2 subunit phosphorylation in CA1 neurons. Anti-γ_2pSer^{327} was specific for pSer^{327} in γ_2 subunit, reacting with phosphorylated wild-type GST-γ_{2S} but not with the mutant GST-γ_{2S} (Ser^{327}-Ala) (Fig. 5*A*). Next, we immunoprecipitated $GABA_A$ receptors from the CA1 extracts. Blot analysis of the immunoprecipitates with anti-γ_2pSer^{327} detected multiple reactive bands, but only the one corresponding to the 51 kDa was selectively blocked by preabsorption with the pSer^{327}-γ_2-peptide antigen (Fig. 5*B*), demonstrating that $GABA_A$ receptor γ_2 subunit is phosphorylated under basal conditions. After induction of LTD of the unitary $GABA_A$R–IPSCs in the CA1 slices, we found that the immunoreactivity to anti-γ_2pSer^{327} was significantly decreased at 5 min (74.2 ± 13.2% over control; $p < 0.05$; $n = 4$) and 30 min (70.9 ± 10.1% over control; $p < 0.05$; $n = 5$; normalized by immunoreactivity to a general anti-γ_2) (Fig. 5*C*). This net dephosphorylation of $GABA_A$ receptor γ_2 subunit was not caused by a tetanus-induced decrease in total protein, because blot analysis showed that the amount of γ_2 subunit was unchanged (Fig. 4*D*).

To assess whether activated CaN is responsible for LTD-dependent dephosphorylation of the $GABA_A$ receptor γ_2 subunit, we examined phosphorylation of the γ_2 subunits in the CaN mice. No change in the basal level of γ_2 subunit phosphorylation was observed in either the CaN control or the mutant mice. However, tetanic stimulation failed to reduce the immunoreactivity to anti-γ_2pSer^{327} in the CaN mutants, as shown in Figure 5*D*, suggesting that CaN-A is necessary for the $GABA_A$ receptor dephosphorylation *in situ*. Moreover, blockade of NMDA receptors by AP-5 inhibited tetanus-induced dephosphorylation of the $GABA_A$ receptors in CaN control mice. We subsequently studied the consequence of blocking other protein phosphatases (PPs) by applying 1 μM calcyculin A, an inhibitor of PP1/2A but not of CaN (Cohen and Cohen, 1989). We found that calyculin A had no effect on the decrease in the immunoreactivity to anti-γ_2pSer^{327} in CaN control mice (Fig. 5*D*).

To identify further specific γ_2 subunit dephosphorylation, but not other subunits of the $GABA_A$ receptors, we labeled the GST-α_1, -β_2, or -γ_2 subunit with ^{32}P *in vitro*. CaN420 specifically caused a decrease in the level of ^{32}P labeling of the GST-γ_{2S} only, and CaN-A immunoprecipitated from LTD-CA1 slices (CaNltd) produced similar results (Fig. 6). In addition, in the presence of γ_2-peptide, neither CaN420 nor CaNltd affects ^{32}P labeling of the GST-γ_{2S} (Fig. 6), indicating that $GABA_A$ receptor γ_{2S} residues 317–332 represent the interacting site of the endogenous CaN-A. Taken together, the above results indicate that activity-dependent CaN-A-$GABA_A$ receptor complex formation enables CaN-A to dephosphorylate the $GABA_A$ receptor γ_{2S} subunit that leads to the induction of LTD of the unitary $GABA_A$R–IPSCs.

Overexpression of CaN-A reduces $mGABA_A$R–IPSCs

We next explored whether the CaN-A-$GABA_A$ receptor complex formation is sufficient for the induction of LTD. We expressed the CaN catalytic domain, CaN-Aα, in the hippocampus of transgenic mice (CN98 mutant mice) (Mansuy et al., 1998; Winder et al., 1998). We affinity precipitated extracts from the CN98 mutant and control CA1 slices using GST-$\alpha_1{}^{334-420}$, -$\beta_2{}^{327-451}$, and -$\gamma_{2S}{}^{317-442}$. We observed that these fusion proteins precipitated CaN-A from the CN98 mutant CA1 extracts but not from control (Fig. 7*A*), showing that overexpressed CaN-A physically interacts with $GABA_A$ receptors.

We then examined whether an interaction of the overexpressed CaN-A and synaptic $GABA_A$ receptor causes a depression of the $GABA_A$R–IPSCs. Pharmacologically isolated (in the presence of 10 μM CNQX and 1 μM TTX), spontaneously miniature $GABA_A$R–IPSCs ($mGABA_A$R-IPSCs) in CA1 pyramidal cells were measured. A significant decrease in mean amplitude of $mGABA_A$R–IPSCs, but not in their frequency, was observed in the CN98 mutant mice (Fig. 7*B*) (63.9 ± 6.6% of the controls; $n = 10$ cells/10 animals; $p < 0.05$). Mean intervals of $mGABA_A$R–IPSCs in the CN98 mutant and control mice were 49.2 ± 7.2 and

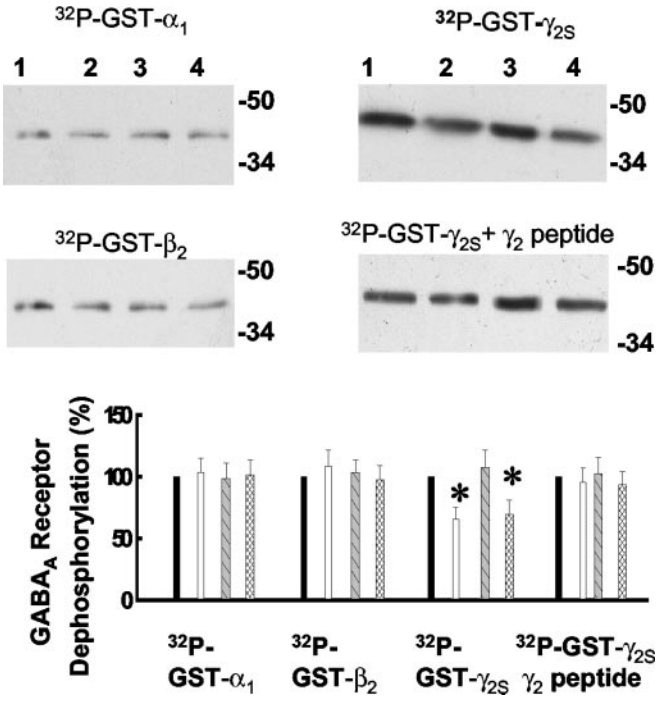

Figure 6. CaN-A and LTD dephosphorylates $GABA_A$ receptor γ_2 subunit. ^{32}P-labeled $GABA_A$ receptor GST fusion proteins (see below) were exposed to 10 μg/ml iCaN420 (heat-inactivated control; *lane 1*) or CaN420 (*lane 2*), CaNctr (control; *lane 3*), or CaNItd (*lane 4*) and analyzed by SDS-PAGE and autoradiography. The extent of ^{32}P labeling for the experiments with iCaN420 (*black bars*), CaN420 (*open bars*), CaNctr (*cross bars*), or CaNItd (*hatched bars*) were quantitated, and normalized to respective controls ($n = 4$; $*p < 0.01$).

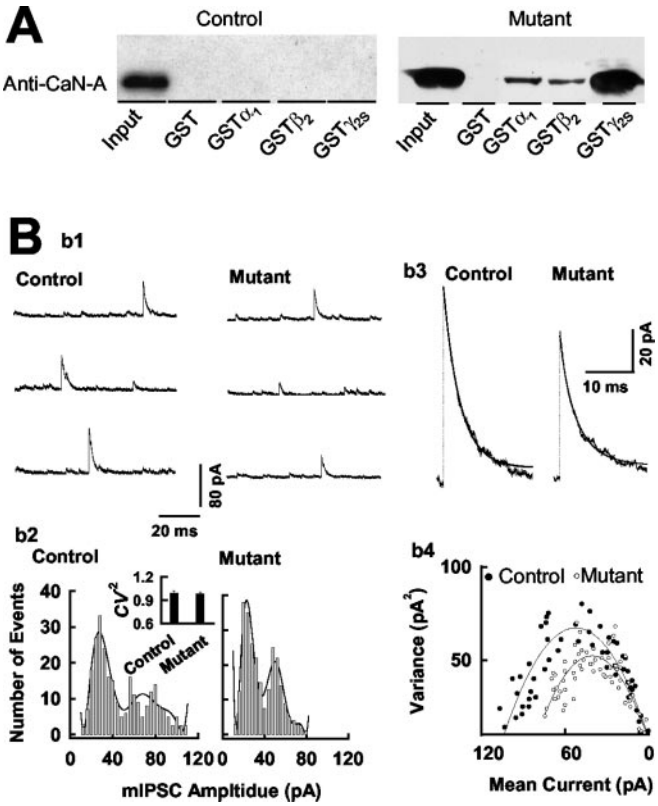

Figure 7. Interaction of CaN-Aα and $GABA_A$ receptors reduces the number of open channels of the synaptic $GABA_A$ receptors. *A*, Affinity precipitation of the CN98 control, or the mutant CA1 slices, with GST-α_1, GST-β_2, GST-γ_{2S}, or GST alone and blots were probed with anti-CaN-A. In the lane marked *Input*, 50 μg of proteins without immunoprecipitation was loaded. Similar results are observed in each of the four experiments. *B*, The number of open channels of the synaptic $GABA_A$ receptors was reduced in CN98 mutant mice. *b1*, Sample traces of mIPSCs in the presence of 1 μM TTX are taken from the experiments with CN98 control or mutant mice. *b2*, The number of events in CN98 control and mutant mice is binned at 4 pA. *Inset*, Summarized coefficient variance (CV^{-2}; $n = 10$ cells). *b3*, Ten to 90% rise time and time constants (τ) of decay in mutant mice were unchanged. *b4*, Current–variance relationships for the mIPSCs are plotted for the experiments with CN98 control or mutant mice.

52.6 ± 6.9 msec ($n = 10$ cells/5 animals; $p > 0.05$), respectively. The distribution of the unitary $GABA_A$R–IPSCs shifted to smaller-amplitude values in the CN98 mutant mice, whereas the *CV* was unchanged (Fig. 7*B*). Using peak-scaled, non-SFA, the properties of synaptically activated $GABA_A$ receptor channels in CN98 mice were determined. A mean γ of 23.6 ± 4.3 pS (mean ± SEM; $n = 10$ cells/10 animals) was obtained in CN98 control mice. This value of γ shows no difference from that in CN98 mutant mice. The synapses in CN98 mice have on average 48 ± 6.1 (mean ± SEM; $n = 10$ cells/5 animals) open channels, and this number decreased to 32 ± 4.2 (mean ± SEM; $n = 10$ cells/10 animals) in CN98 mutant mice, indicating that a decrease in the number of the synaptically activated $GABA_A$ receptor channels is responsible for the reduced m$GABA_A$R–IPSCs in CN98 mutant mice.

CaN-A-induced responses and LTD occlude each other

If a reduction of the $GABA_A$R–IPSCs by CaN-A mimics the features of tetanus-induced LTD, then LTD and the $GABA_A$R–IPSC reduction by CaN-A may mask each other. This was initially investigated by comparing the current–variance relationship of spontaneously occurring IPSCs (sIPSCs; without TTX) 30 min after tetanus in CN98 control mice with that in mutant mice (Fig. 8*A*). Estimated sIPSC rise times in control and the CN98 mutant mice were 0.22 ± 0.02 and 0.24 ± 0.03 msec, respectively. The decay time constants were 3.18 ± 0.21 msec in control compared 3.21 ± 0.18 msec in the CN98 mutant mice. The channel conductance (γ) of the synaptic $GABA_A$ receptors in the CN98 mutant mice was 24.1 ± 3.2 pS, similar to that (22.9 ± 2.8 pS) in control mice (Fig. 8*A*). In contrast, the number (N_o) of open channels of the synaptic $GABA_A$ receptors was reduced in CN98 mutant mice; the synapses in control mice have on average 53 ± 8.2 (mean ± SEM) open channels, and this number decreased to 39 ± 6.4 (mean ± SEM) in the CN98 mutant mice. No reduction of the N_o after tetanus was observed in CN98 mutant mice, whereas tetanus did produce a decrease in the number of synaptically activated $GABA_A$ receptor channels in CN98 control mice. Thus, CaN-A caused a decrease in the number of the synaptic $GABA_A$ receptor channels that appeared to occlude the tetanus effect.

Second, we examined the dependence of LTD on the concentration of exogenous CaN-Aα. A consistent threshold for the depression of the unitary $GABA_A$R-IPSCs was detected by application of CaN420 (2 μg/ml), with a maximum depression near 10 μg/ml. CaN420 (10 μg/ml) was then applied directly into the CA1 pyramidal cells through the patch electrodes. The amplitude of the unitary $GABA_A$R–IPSCs decreased to 58.4 ± 6.7% of baseline ($n = 6$ recordings). In contrast, heat-inactivated CaN420 (iCaN420) had no effect (Fig. 8*B*). Moreover, application of CaN420 did not alter the reversal potentials, as shown by the current–voltage curves for peak amplitude of the unitary $GABA_A$R–IPSCs in Figure 8*B*. The data demonstrate that activated CaN reduces the peak amplitude of unitary $GABA_A$R–IPSCs, with no change in driving force.

In other experiments, tetanus produced a reduction of the

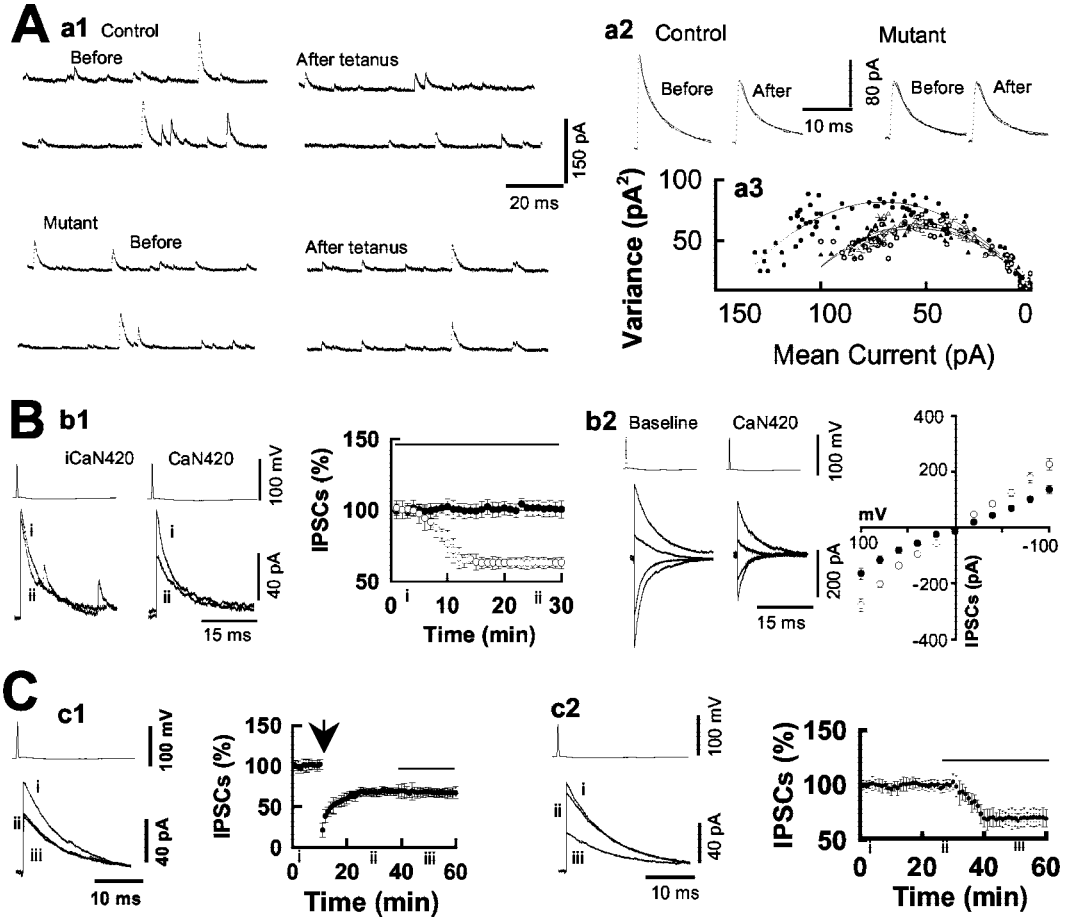

Figure 8. CaN-A-induced depression and LTD occluded each other. *A*, Effect of tetanus on spontaneous IPSCs. Single (*a1*) or averaged (20 consecutive responses) (*a2*) traces are taken from the experiments with the CN98 control or mutant mice. *a3*, Current–variance relationships for spontaneous IPSCs are plotted before (*filled symbols*) and 20 min after tetanus (*open symbols*) from the experiments with the CN98 control (*circles*) or the mutant mice (*triangles*). The data points are fitted by a parabolic function. *B*, CaN420 reduces amplitudes of the unitary $GABA_A$R–IPSCs. *b1*, The traces are single action potentials (*top*) and averaged 10 consecutive unitary $GABA_A$R–IPSCs (*bottom*) taken at the time indicated by the *letters*. Normalized unitary $GABA_A$R–IPSCs for the recordings with 10 μg/ml iCaN420 (*filled circles*; $n = 5$) or 10 μg/ml CaN420 (*open circles*; $n = 6$) are plotted. *b2*, Single action potential and superimposed unitary $GABA_A$R–IPSCs at -60 to $+60$ mV (40 mV increment) recorded with high Cl^- (*top*). Current–voltage relationships ($n = 4$) are taken from 5 min (*Baseline*; *open circles*) and 20 min after starting recording (*filled circles*). *C*, Effects of tetanus on CaN420 action. Single action potentials (*top*) and averaged 10 consecutive unitary $GABA_A$R–IPSCs (*bottom*) are taken at the time indicated by the *letters*. Normalized amplitudes of the unitary $GABA_A$R–IPSCs when tetanus (*arrowhead*) was delivered 10 min after the start of recording (*c1*) or without tetanus (*c2*) are plotted. CaN420 (10 μg/ml) was actively perfused during the period indicated by the *horizontal bars*.

unitary $GABA_A$R–IPSCs, but there was no further decrease when CaN420 was applied intracellularly (Fig. 8*C*). On the other hand, in cells not conditioned by tetanus, perfusion of CaN420 at the same time after beginning recording caused a decrease in the unitary $GABA_A$R–IPSCs that reached a stable level at $63.8 \pm 7.9\%$ of the baseline ($n = 6$ cells). Thus, the CaN-A-induced reduction of the unitary $GABA_A$R–IPSCs and LTD occluded each other, indicating an overlapping mechanism of action.

Discussion

Our analysis of the molecular mechanisms contributing to LTD of the unitary $GABA_A$R–IPSCs revealed a novel postsynaptic event: an activity-dependent physical and functional interaction between CaN-A and the $GABA_A$ receptor-γ_2 subunit permits a rapid and sustained reduction of inhibitory synaptic strength at individual CA1 synapses. Furthermore, our results indicate that the CaN–$GABA_A$ receptor complex formation occurs only at synapses conditioned by activation of postsynaptic NMDA receptors. We determined that activated endogenous CaN was recruited into the $GABA_A$ receptors at CA1 inhibitory synapses via a direct binding with the γ_{2S} subunit, because a synthesized γ_2-peptide that encodes residues 317–332 of the γ_{2S} subunit prevented CaN interaction with $GABA_A$ receptors. Because intracellular application of the γ_2-peptide directly into the postsynaptic neurons inhibited the induction of LTD at CA1 individual inhibitory synapses, the most parsimonious explanation for our results is that activation of NMDA receptors results in increased Ca^{2+} entry, which activates CaN, and drives the activated CaN to dephosphorylate postsynaptic $GABA_A$ receptors, leading to a downregulation of $GABA_A$ receptor function.

Although we did not directly rule out presynaptic release properties during LTD, similar values of the coefficient variance of the evoked unitary IPSCs and spontaneous IPSCs before versus after the induction of LTD were observed. Using peak-scaled, non-SFA, our data showed that the reduced number of the synaptically activated $GABA_A$ receptor channels accounts for LTD at CA1 inhibitory synapses. Thus, taken together, our biochemical and electrophysiological data are not consistent with the presynaptic locus of NMDA receptor-dependent LTD of the unitary $GABA_A$R–IPSCs in CA1 neurons.

CaN is known to play a role in the induction of LTD of excitatory transmission in CA1 neurons (Kirkwood and Bear, 1994; Mulkey et al., 1994). Consistent with these pharmacological studies, a recent study in the knock-out mice that lack CaN regulatory domain B1 showed that the induction of LTD at CA1 excitatory synapses was impaired (Zeng et al., 2001). The mechanisms by which the CaN-dependent signaling pathway participates in LTD at CA1 excitatory synapses are thought to involve the CaN-dependent activation of PP1 by inactivating I-1, a PP1 inhibitor (Lisman and Zhabotinsky, 2001). Consistent with this idea, the postsynaptic injection of I-1 peptides that mimics the phosphorylated, activated state of I-1 blocks the induction of LTD of excitatory transmission in CA1 pyramidal cells (Mulkey et al., 1994). From our results using GST fusion proteins of the subunit intracellular domains, we suggest that activated CaN is directly targeted to the phospho-Ser^{327} of the γ_{2S} subunit. Therefore, low-frequency stimulation activates the CaN-dependent PP1 pathway that leads to the induction of LTD of excitatory transmission, whereas a brief high-frequency stimulation drives an activated CaN directly onto the $GABA_A$ receptors, leading to the induction of LTD at CA1 inhibitory synapses.

Among the mechanisms proposed for modification of $GABA_A$ receptor activity, one of the simplest is a change in the number of $GABA_A$ receptors in the postsynaptic membrane. There is extensive evidence showing that the $GABA_A$ receptor γ_2 subunit plays a critical role in postsynaptic membrane trafficking as well as in synaptic targeting of $GABA_A$ receptors. For example, the number of synaptic $GABA_A$ receptors was decreased in cerebral cortex of mice lacking the γ_2 subunit (Essrich et al., 1998). The γ_2 subunits of $GABA_A$ receptors interact differentially with diverse intracellular molecules including GABARAP (Nymann-Andersen et al., 2002), α-adaptin (Kittler et al., 2000), and Src (Brandon et al., 2001), all of which have been implicated in synaptic targeting of $GABA_A$ receptors. For example, in cultured hippocampal neurons, the α-adaptin-γ_2 subunit association disrupts the clathrin-dependent $GABA_A$ receptor endocytosis. Therefore, it is possible that CaN-A interferes with the α-adaptin-γ_2 subunit interaction to regulate the number of functional $GABA_A$ receptors in the inhibitory postsynaptic sites. However, our observation show that the γ_2-peptide that prevents CaN-A-$GABA_A$ receptor complex formation did not change the α-adaptin-$GABA_A$ receptor association, indicating that CaN acts via direct CaN-A–γ_2 subunit interactions rather than as an adaptin substrate. Interestingly, clathrin-mediated endocytosis is involved in the expression of cerebellar LTD at excitatory synapses (Wang and Linden, 2000). It will be of importance to explore whether CaN regulation of $GABA_A$ receptors is mediated by the clathrin-dependent $GABA_A$ receptor internalization. The internal versus surface expression of $GABA_A$ receptors in the postsynaptic sites needs to be examined to determine CaN-mediated $GABA_A$ receptor trafficking to and from the cell surface that is therefore likely to be an important mechanism for expression of LTD at inhibitory synapses. In addition to adaptin, there has been a report that tyrosine kinase Src modulates neuronal as well as recombinant $GABA_A$ receptors to enhance receptor channel activity (Moss et al., 1995). Src kinase also phosphorylates both Y^{365} and Y^{367} residues of the γ_{2L} (long form) subunit (Moss et al., 1995). By specifically blocking the association of Src with the $GABA_A$ receptor γ_2 subunit (Fig. 3*E*), CaN may act as a competitive inhibitor of Src to downregulate $GABA_A$ receptor function. Clearly, further studies will be needed to clarify the interaction of CaN and Src kinase with regard to $GABA_A$ receptor function.

There is extensive evidence showing that PKC phosphorylates $GABA_A$ receptors and increases the peak amplitude of mIPSCs recorded from hippocampal granule cells (Poisbeau et al., 1999) (but see Connolly et al., 1999). PKC also enhances the channel activity of recombinant $GABA_A$ receptors expressed in the L929 cell line (Lin et al., 1994, 1996). A recent study shows that activation of PP1 decreases in phosphorylation of $Ser^{657/660}$ on the catalytic domain of PKCα and PKCβ_{II} (Thiels et al., 2000). This decrease in PKC phosphorylation is associated with a decrease in PKC activity. Thus, CaN may act through the PP1 pathway to downregulate PKC leading to the downregulation of $GABA_A$ receptor function for inducing LTD at CA1 inhibitory synapses. Because the $GABA_A$ receptor subunit combination and the receptor density expressed in CA1 pyramidal cells are heterogeneous (Pettit and Augustine, 2000), the effect of PKC phosphorylation of the $GABA_A$ receptor on its channel activity may depend on the receptor types under study. Therefore, whether the CaN–PKC pathway is involved in LTD at CA1 inhibitory synapses needs to be clarified in hippocampal slices. Further studies will use the strategies and protocols established in this study to determine how protein kinases are targeted to the synaptic $GABA_A$ receptors in synaptic plasticity. The final illustration of the cellular and molecular mechanisms underlying bidirectional regulation of $GABA_A$ receptors mediated by kinases and phosphatases in synaptic plasticity can teach us much about what kinds of molecules are needed to build arrays of the $GABA_A$ receptor regulations.

CaN is reported to modulate the channel kinetics of the $GABA_A$ receptors in cultured neurons (Jones and Westbrook, 1997). However, we found that there were no changes of the unitary $GABA_A$R–IPSC rise times or their decay time constants after activation of CaN. The different observations could be attributed to the fact that in previous studies, reduced decay times of IPSC were caused by inhibition of endogenous CaN, which is generally dependent on the basal level of CaN activity. In hippocampal slices, however, we found that there were no physical and functional interactions of CaN and $GABA_A$ receptors at basal CA1 inhibitory synapses. Therefore, it is possible that enzymatic regulation of synaptic receptors in cultured neurons is different from that in acute isolated neurons in the slices. Consistent with this idea, two other previous studies show that the activated but not basal level of CaN reduces the peak amplitude of whole-cell $GABA_A$ receptor currents in acute isolated hippocampal neurons (Stelzer and Shi, 1994; Chen and Wong, 1995).

Much of the difficulty in assigning changes at the level of individual inhibitory synapses is that the IPSCs, originating from feed-forward (Alger and Nicoll, 1982) as well as feed-back activation of the CA1 interneurons (Lacaille and Schwartzkroin, 1988) by the Schaffer-collateral stimulation, are polysynaptic and thus obscure any link between properties of IPSCs and the efficacy of individual inhibitory synapses. Conventionally, the $GABA_A$R–IPSCs in CA1 pyramidal neurons are studied under conditions in which excitatory glutamate receptors are blocked. This manipulation, however, fails to account for NMDA receptor-dependent intracellular events that are essential for both $GABA_A$ receptor regulation and the initiation of sustained change in inhibitory synaptic strength. Here, we established double whole-cell patch-clamp recordings by which we monitored the unitary $GABA_A$R–IPSCs between identified pairs of CA1 interneurons and the innervated pyramidal cells from hippocampal slices. Using both genetic manipulations and biochemical assays, we determined the mechanisms for excitatory activity-dependent LTD at inhibitory synapses. These data demonstrate a previously

unknown molecular mechanism by which individual GABAergic synapses alter their efficacy in CA1 neurons of the hippocampus. Because inhibitory synaptic strength is critical for the control of networks within the brain (Ben-Ari and Represa, 1990), our results may suggest a CaN-dependent cellular substrate of learning and memory.

References

Abraham WC, Gustafsson B, Wigstrom H (1987) Long-term potentiation involves enhanced synaptic excitation relative to synaptic inhibition in guinea-pig hippocampus. J Physiol (Lond) 394:367–380.

Aizenman CD, Manis PB, Linden DJ (1998) Polarity of long-term synaptic gain change is related to postsynaptic spike firing at a cerebellar inhibitory synapse. Neuron 21:827–835.

Alger BE, Nicoll RA (1982) Feed-forward dendritic inhibition in rat hippocampal pyramidal cells studied *in vitro*. J. Physiol (Lond) 328:105–123.

Ali DW, Salter MW (2001) NMDA receptor regulation by Src kinase signalling in excitatory synaptic transmission and plasticity. Curr Opin Neurobiol 11:336–342.

Andersen P, Lømo T (1968) Inhibitory synapses. In: Structure and function of inhibitory neuronal mechanisms (von Euler C, Skoglund S, Soderberg U, eds), pp 335–342. Oxford: Pergamon.

Auger C, Marty A (1997) Heterogeneity of functional synaptic parameters among single release sites. Neuron 19:139–150.

Ben-Ari Y, Represa A (1990) Brief seizure episodes induce long-term potentiation and mossy fiber sprouting in the hippocampus. Trends Neurosci 13:312–318.

Bliss TV, Collingridge GL (1993) A synaptic model of memory: long-term potentiation in the hippocampus. Nature 361:31–39.

Brandon NJ, Uren JM, Kittler JT, Wang H, Olsen R, Parker PJ, Moss SJ (1999) Subunit-specific association of protein kinase C and the receptor for activated C kinase with GABA type A receptors. J Neurosci 19:9228–9234.

Brandon NJ, Delmas P, Kittler JT, McDonald BJ, Sieghart W, Brown DA, Smart TG, Moss SJ (2000) $GABA_A$ receptor phosphorylation and functional modulation in cortical neurons by a protein kinase C-dependent pathway. J Biol Chem 275:38856–38862.

Brandon NJ, Delmas P, Hill J, Smart TG, Moss SJ (2001) Constitutive tyrosine phosphorylation of the $GABA_A$ receptor γ2 subunit in rat brain. Neuropharmacology 41:745–752.

Chen QX, Wong RK (1995) Suppression of $GABA_A$ receptor responses by NMDA application in hippocampal neurons acutely isolated from the adult guinea-pig. J Physiol (Lond) 482:353–362.

Cohen P (1989) The structure and regulation of protein phosphatases. Annu Rev Biochem 58:453–508.

Cohen P, Cohen PTW (1989) Protein phosphatases come of age. J Biol Chem 264:21435–21438.

Connolly CN, Kittler JT, Thomas P, Uren JM, Brandon NJ, Smart TG, Moss SJ (1999) Cell surface stability of gamma-aminobutyric acid type A receptors. Dependence on protein kinase C activity and subunit composition. J Biol Chem 274:36565–36572.

De Koninck Y, Mody I (1994) Noise analysis of miniature IPSCs in adult rat brain slices: properties and modulation of synaptic $GABA_A$ receptor channels. J Neurophysiol 71:1318–1334.

Edwards FA, Konnerth A, Sakmann B (1990) Quantal analysis of inhibitory synaptic transmission in the dentate gyrus of rat hippocampal slices: a patch-clamp study. J Physiol (Lond) 430:213–249.

Essrich C, Lorez M, Benson JA, Fritschy JM, Luscher B (1998) Postsynaptic clustering of major GABAA receptor subtypes requires the gamma 2 subunit and gephyrin. Nat Neurosci 1:563–571.

He TC, Jiang N, Zhuang H, Wojchowski DM (1995) Erythropoietin-induced recruitment of Shc via a receptor phosphotyrosine-independent, Jak2-associated pathway. J Biol Chem 270:11055–11061.

Jones MV, Westbrook GL (1997) Shaping of IPSCs by endogenous calcineurin activity. J Neurosci 17:7626–7633.

Kirkwood A, Bear MF (1994) Homosynaptic long-term depression in the visual cortex. J Neurosci 14:3404–3412.

Kittler JT, Delmas P, Jovanovic JN, Brown DA, Smart TG, Moss SJ (2000) Constitutive endocytosis of $GABA_A$ receptors by an association with the adaptin AP2 complex modulates inhibitory synaptic currents in hippocampal neurons. J Neurosci 20:7972–7977.

Lacaille JC, Schwartzkroin PA (1988) Stratum lacunosum-moleculare interneurons of hippocampal CA1 region. II. Intrasomatic and intradendritic recordings of local circuit synaptic interactions. J Neurosci 8:1411–1424.

Lin YF, Browning MD, Dudek EM, MacDonald RL (1994) Protein kinase C enhances recombinant bovine $\alpha1\beta1\gamma2L$ GABAA receptor whole-cell currents expressed in L929 fibroblasts. Neuron 13:1421–1431.

Lin YF, Angelotti TP, Dudek EM, Bowing MD, MacDonald RL (1996) Enhancement of recombinant $\alpha1\beta1\gamma2L$ γ-aminobutyric acid A receptor whole-cell currents by protein kinase C is mediated through phosphorylation of both $\beta1$ and $\gamma2L$ subunits. Mol Pharmacol 50:185–195.

Lisman JE, Zhabotinsky AM (2001) A model of synaptic memory: a CaMKII/PP1 switch that potentiates transmission by organizing an AMPA receptor anchoring assembly. Neuron 31:191–201.

Liu F, Wan Q, Pristupa Z, Wang YT, Niznik HB (2000) Direct protein-protein binding enables reciprocal dopamine D5 and $GABA_A$ receptor cross-talk. Nature 403:274–280.

Lu YM, Roder JC, Davidow J, Salter MW (1998) Src activation in the induction of long-term potentiation in CA1 hippocampal neurons. Science 279:1363–1367.

Lu YM, Mansuy IM, Kandel ER, Roder J (2000) Calcineurin-mediated LTD of GABAergic inhibition underlies the increased excitability of CA1 neurons associated with LTP. Neuron 26:197–205.

MacDonald RL, Olsen RW (1994) $GABA_A$ receptor channels. Annu Rev Neurosci 17:569–602.

Malenka RC, Nicoll RA (1999) Long-term potentiation—a decade of progress? Science 285:1870–1874.

Malinow R, Mainen ZF, Hayashi Y (2000) LTP mechanisms: from silence to four-lane traffic. Curr Opin Neurobiol 10:352–357.

Malleret G, Haditsch U, Genoux D, Jones MW, Bliss TV, Vanhoose AM, Weitlauf C, Kandel ER, Winder DG, Mansuy IM (2001) Inducible and reversible enhancement of learning, memory, and long-term potentiation by genetic inhibition of calcineurin. Cell 104:675–686.

Mansuy IM, Mayford M, Jacob B, Kandel ER, Bach ME (1998) Restricted and regulated overexpression reveals calcineurin as a key component in the transition from short-term to long-term memory. Cell 92:39–49.

McKernan RM, Whiting PJ (1996) Which GABAA-receptor subtypes really occur in the brain? Trends Neurosci 19:139–143.

Moss SJ, Doherty CA, Huganir RL (1992) Identification of the cAMP-dependent protein kinase and protein kinase C phosphorylation sites within the major intracellular domains of the beta 1, gamma 2S, and gamma 2L subunits of the gamma-aminobutyric acid type A receptor. J Biol Chem 267:14470–14476.

Moss SJ, Gorrie GH, Amato A, Smart TG (1995) Modulation of $GABA_A$ receptors by tyrosine phosphorylation. Nature 377:344–348.

Mulkey RM, Endo S, Shenolikar S, Malenka RC (1994) Involvement of a calcineurin/inhibitor-1 phosphatase cascade in hippocampal long-term depression. Nature 369:486–488.

Nusser Z, Hajos N, Somogyi P, Mody I (1998) Increased number of synaptic $GABA_A$ receptors underlies potentiation at hippocampal inhibitory synapses. Nature 395:172–177.

Nymann-Andersen J, Wang H, Chen L, Kittler JT, Moss SJ, Olsen RW (2002) Subunit specificity and interaction domain between GABA(A) receptor-associated protein (GABARAP) and GABA(A) receptors. J Neurochem 80:815–823.

Otis TS, De Koninck Y, Mody I (1994) Lasting potentiation of inhibition is associated with an increased number of gamma-aminobutyric acid type A receptors activated during miniature inhibitory postsynaptic currents. Proc Natl Acad Sci USA 91:7698–7702.

Paulsen O, Moser EI (1998) A model of hippocampal memory encoding and retrieval: GABAergic control of synaptic plasticity. Trends Neurosci 21:273–278.

Perrino B, Ng LY, Soderling TR (1995) Calcium regulation of calcineurin phosphatase activity by its B subunit and calmodulin. Role of the autoinhibitory domain. J Biol Chem 270:340–346.

Pettit DL, Augustine GJ (2000) Distribution of functional glutamate and GABA receptors on hippocampal pyramidal cells and interneurons. J Neurophysiol 84:28–38.

Poisbeau P, Cheney MC, Browning MD, Mody I (1999) Modulation of synaptic $GABA_A$ receptor function by PKA and PKC in adult hippocampal neurons. J Neurosci 19:674–683.

Silver RA, Momiyama A, Cull-Candy SG (1998) Locus of frequency-dependent depression identified with multiple-probability fluctuation analysis at rat climbing fibre-Purkinje cell synapses. J Physiol (Lond) 510:881–902.

Stelzer A, Shi H (1994) Impairment of GABAA receptor function by *N*-methyl-D-aspartate-mediated calcium influx in isolated CA1 pyramidal cells. Neuroscience 62:813–828.

Stelzer A, Slater N, Bruggencate G (1987) Activation of NMDA receptors blocks GABAergic inhibition in an in vitro model of epilepsy. Nature 326:698–701.

Thiels E, Kanterewicz BI, Knapp LT, Barrionuevo G, Klann E (2000) Protein phosphatase-mediated regulation of protein kinase C during long-term depression in the adult hippocampus *in vivo*. J Neurosci 20:7199–7207.

Thompson SM (1994) Modulation of inhibitory synaptic transmission in the hippocampus. Prog Neurobiol 42:575–609.

Thompson SM, Gahwiler BH (1989) Activity-dependent disinhibition. I. Repetitive stimulation reduces IPSP driving force and conductance in the hippocampus *in vitro*. J Neurophysiol 61:501–511.

Traynelis SG, Silver RA, Cull-Candy SG (1993) Estimated conductance of glutamate receptor channels activated during EPSCs at the cerebellar mossy fiber-granule cell synapse. Neuron 11:279–289.

Wang YT, Linden DJ (2000) Expression of cerebellar long-term depression requires postsynaptic calthrin-mediated endocytosis. Neuron 25:635–647.

Winder DG, Sweatt JD (2001) Roles of serine/threonine phosphatases in hippocampal synaptic plasticity. Nat Rev 2:461–474.

Winder DG, Mansuy IM, Osman M, Moallem TM, Kandel ER (1998) genetic and pharmacological evidence for a novel intermediate phase of long-term potentiation suppressed by calcineurin. Cell 92:25–37.

Zeng H, Chattarji S, Barbarosie M, Rondi-Reig L, Philipot BD, Miyakawa T, Bear MF, Tonegawa S (2001) Forebrain-specific calcineurin knockout selectively impair bi-directional synaptic plasticity and working/episodic-like memory. Cell 107:617–629.